

# NOVEL 2.5D LAYERED MODEL TO SIMULATE DISCRETE CRACK GROWTH IN CONCRETE SPECIMENS

**BENIAMIN KONDYS\* AND JERZY BOBIŃSKI\***

\* Gdańsk University of Technology, Faculty of Civil and Environmental Engineering  
11/12 Gabriela Narutowicza Street, 80-233 Gdańsk, Poland  
e-mail: beniamin.kondys@pg.edu.pl, jerzy.bobinski@pg.edu.pl

**Key words:** Concrete, Cracks, Mesostructure, Finite Element Method, Cohesive Elements

**Abstract:** The paper presents a novel 2.5D model to simulate concrete or reinforced concrete specimens. The main idea of this approach is to define the set of 2D plane models extracted from the 3D model or specimen's microtomography ( $\mu$ CT) scan along selected direction. The definition of several cut planes allows for defining different material and geometrical configurations (e.g. different mesostructure topology and the inclusion of reinforced bars). These plane cuts can be analysed independently as simple standalone 2D models, but they also can interact with neighbouring plane or planes. Interaction between planes is adhered to by adding a set of horizontal and vertical springs with a prescribed stiffness. Consequently, the proposed approach is still a two-dimensional model but is capable of mimicking the behaviour of three-dimensional specimens. A detailed description of the method is provided, along with some preliminary results, and the difference between pure 2D simulations and the 2.5D approach is outlined.

## 1 INTRODUCTION

Accurate simulations of concrete and reinforced concrete specimens is a quite challenging problem. The first reason is the complex nonlinear behaviour of concrete itself. Fundamentally, it is manifested by the presence of cracks in which strains/deformations are concentrated. These regions are very thin and require relatively fine finite element (FE) meshes to accurately describe their topology [1].

The second source of complexity comes from the observation level. On the macroscale, concrete can be considered a homogeneous material, which allows for defining relatively coarse FE meshes [2-3]. Only in reinforced concrete (RC) specimens this homogeneity is disrupted by bars and stirrups. At the mesoscale, however, different phases like aggregates, interfacial transition zones (ITZs), cement matrix and air voids can be distinguished. Given their dimensions, it is

necessary to apply a fine mesh discretisation technique once more [4-7].

Finally, the dimensional aspect is also important. In reality, all specimens possess three-dimensional characteristics. In structural analysis, several simplified approaches are commonly used: rods, beams, plates or shells. In research calculations, if the analysis of cracks is important, usually at least two-dimensional models (under plane stress or plane strain assumption) are employed [4-8]. When the mesostructure of the concrete is defined and reinforcement is present, such an approach may seem to be too simplistic to obtain results consistent with experiments. In such cases, the three-dimensional model should be formulated, but this would require an enormous number of finite elements [9] and finds its application primarily in very small models [10].

In the presented paper, a compromise between 2D and 3D modelling is proposed. This new approach is based on a set of 2D

layers extracted from a 3D specimen along the predefined direction. The interaction between neighbouring layers is imposed via horizontal and vertical springs with prescribed stiffness. Interacting 2D layers may have different topologies of mesostructure and FE meshes which allow incorporating connection between layers with/without reinforced bars. Concrete is modelled as a heterogenous mesoscale material (cement matrix, aggregates, air voids, rebars, ITZs surrounding aggregates and rebars) with cracks introduced in a discrete approach as a strong discontinuity by cohesive elements. Cohesive elements with traction-separation constitutive law and material parameters varying of neighbouring bulk elements (cement-cement, cement-aggregates i.e. ITZs, and cement-rebar interfaces) are inserted in the bulk mesh by MATLAB script [11] to implement the possibility of initiation and propagation discrete cracking.

## 2 METHOD

### 2.1 2.5D model

From a 3D model or 3D specimen's  $\mu$ CT scan variable number of cut planes are defined along the chosen direction (Figure 1). The out-of-plane thickness of each cut is adjusted according to the number of planes and the total thickness of specimen. The 2.5D model similar to the standard 2D model is intended to simulate only 'in-plane' loadings (i.e. without torsion, or biaxial bending). Boundary conditions and prescribed displacements are separately defined on each 2D plane. Finally, 2D planes are connected to each other by a set of springs.

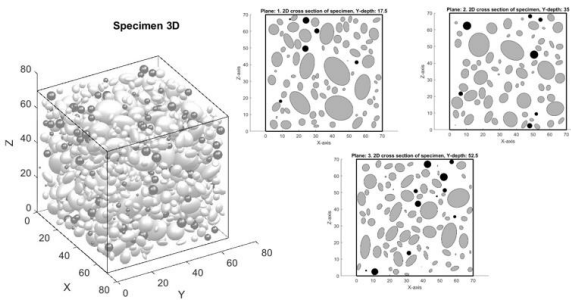


**Figure 1:** 3D mesoscale specimen model and 3 different cut planes.

### 2.2 Springs

The proposed methodology addresses the issue of mesh intersection and coupling through a four-stage process. As illustrated in Figure 2, the overlapping meshes are identified through the planar intersection, where Mesh A and Mesh B are superimposed. The subsequent step in the procedure is to identify the pairs of overlapping elements. (Figure 2C).

The intersection procedure is followed by a node connection strategy, depicted in Figure 3, where the overlapping area ( $A_{inter}$ ) is identified, and new nodes (A4/B4) are inserted at its centroid position. These nodes are then connected to their respective element nodes using multi-point constraints (MPC) - node A4 is linked to the nodes of Mesh A element, while B4 is connected to the nodes of Mesh B element. Furthermore, the configuration of the spring elements in both the X and Y directions between nodes A4 and B4 ensures a mechanical coupling while allowing for the accommodation of relative deformation.

The spring stiffness between coupled nodes is derived from the finite element model parameters, where the total spring constant  $K_i$  is calculated as the product of the overlapping area and specific surface stiffness:

$$K_i = \frac{A_{inter}}{t} \cdot k_i \quad (1)$$

where  $t$  means the distance between layers (average out-of-plane thickness) and the specific surface stiffness  $k_i$  is determined by the material properties of the connected elements:

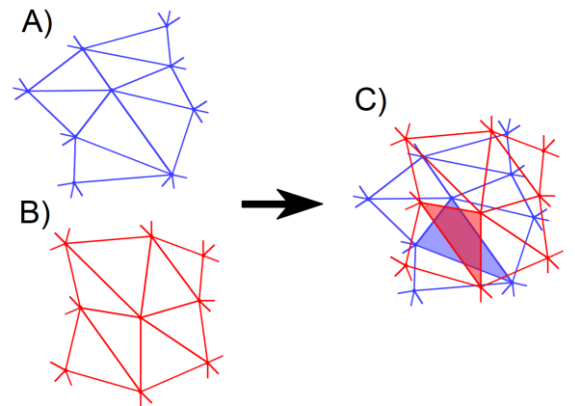


**Figure 2:** A) Mesh A; B) Mesh B; C) Mesh A and Mesh B overlapped in one plane with highlighted one pair of overlapping elements.

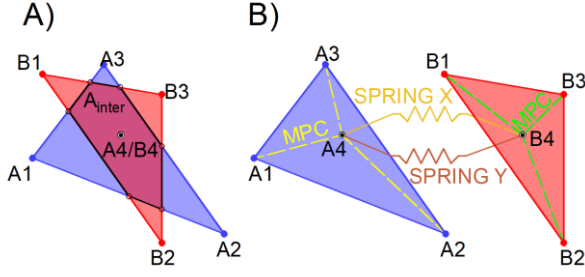


**Figure 3:** A) Intersection of elements overlapping areas ( $A_{inter}$ ) and new nodes A4/B4 in the centroid of the  $A_{inter}$ ; B) New nodes A1/B4 attached to existing nodes using multi-point constraints (MPC) and X and Y springs between nodes A4 and B4.

$$k_i = C \cdot E \quad (2)$$

where  $C$  is a constant and  $E$  is the Young modulus. When a spring connects two elements made of different materials, the following relationship may be alternatively applied:

$$k_i = C \cdot \sqrt{E_A E_B} \quad (3)$$

where  $E_A$  and  $E_B$  represent the elastic moduli assigned to the respective intersecting elements. This formulation ensures that the coupling stiffness appropriately reflects both the geometric intersection and material characteristics of the connected regions.

### 2.3 Material definition

In general, for the 2.5D method, any constitutive law can be applied to describe cracks in concrete, including both continuous and discontinuous approaches e.g., elastoplastic models (utilising plasticity theory and accounting for permanent deformations), damage models (based on material stiffness degradation variables, including material models used in discrete methods such as CZM (Cohesive Zone Model) and XFEM (eXtended Finite Element Method)), as well as coupled approaches. Therefore, the choice of constitutive approach does not affect the formulation of the springs (Section 2.2) and, consequently, the behaviour of the 2.5D model described in Section 2.1.

Within this work to model crack initiation and propagation, the CZM method was used,

where discrete cracks are implemented to the FEA model by the insertion of interface cohesive elements governed by the traction-separation law between bulk elements exhibiting linear elastic behaviour.

The traction-separation law relates traction stresses to relative displacements (Figure 4), incorporating both normal  $t_n$  and tangential  $t_s$  components according to the Hilleborg fictitious crack model [12]. For the normal direction,  $t_n$  evolves based on crack opening  $\delta_n$ :

$$t_n = \begin{cases} \sigma_n, & \sigma_n \leq f_t \\ f(\delta), & \sigma_n > f_t \end{cases} \quad (4)$$

where  $f_t$  is the tensile strength, and  $f(\delta)$  is the softening function. The traction stress vector depends on interface stiffness  $k_n$ ,  $k_s$ , and relative displacements  $\delta_n$ ,  $\delta_s$ :

$$\begin{bmatrix} t_n \\ t_s \end{bmatrix} = \begin{bmatrix} k_n & 0 \\ 0 & k_s \end{bmatrix} \begin{bmatrix} \delta_n \\ \delta_s \end{bmatrix} \quad (5)$$

Crack initiation occurs when the quadratic stress criterion is met:

$$\left\{ \frac{\langle t_n \rangle}{t_{n0}} \right\}^2 + \left\{ \frac{t_s}{t_{s0}} \right\}^2 = 1 \quad (6)$$

with  $t_{n0}$ ,  $t_{s0}$  as critical stresses, where  $\langle \cdot \rangle$  denotes ramp function:

$$\langle x \rangle = \max\{0; x\} \quad (7)$$

ensuring negative (compressive) stresses are excluded.

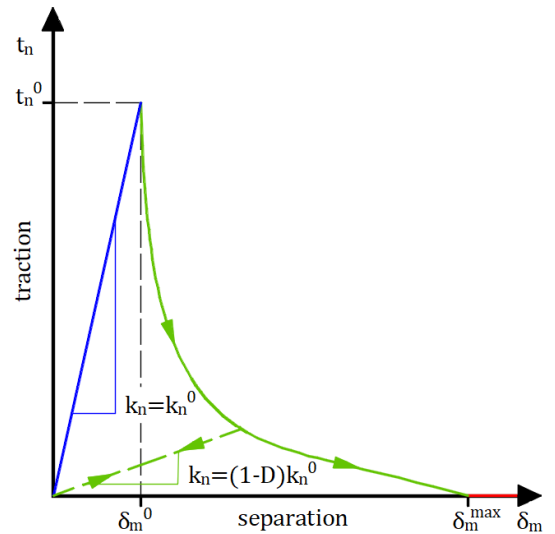


**Figure 4:** Exponential softening curve for traction-separation law for pure tension mode.

Once initiated, stiffness degrades according to the damage variable  $D$ , in this case exponentially defined:

$$D = 1 - \left\{ \frac{\delta_m^0}{\delta_m^{\max}} \right\} \left\{ 1 - \frac{1 - \exp \left[ -\alpha \left( \frac{\delta_m^{\max} - \delta_m^0}{\delta_m^f - \delta_m^0} \right) \right]}{1 - \exp(-\alpha)} \right\} \quad (8)$$

Here  $\delta_m^0$  is the effective relative displacement at crack initiation,  $\delta_m^f$  is the displacement at complete stiffness degradation,  $\delta_m^{\max}$  is the maximum effective relative displacement during loading, and  $\alpha$  is a material parameter controlling the damage evolution rate. This relationship is valid while:

$$\delta_m^{\max} \leq \delta_m^f \quad (9)$$

otherwise:

$$D = 1.0 \quad (10)$$

When the initiation criterion described by Equation (6) is fulfilled in a particular cohesive element, the stiffness of that element begins to degrade. This softening effect is captured through the reduction of interface stiffness:

$$k_n = (1 - D)k_{n0} \quad (11)$$

and:

$$k_s = (1 - D)k_{s0} \quad (12)$$

where  $k_{n0}$  and  $k_{s0}$  represent the initial stiffness in the normal and tangential directions, respectively.

This model ensures that stiffness degradation begins upon satisfying the crack initiation criterion and evolves as a function of effective relative displacement, with normal and tangential components coupled through the traction-separation law.

For bulk/solid finite elements linear elastic stress-strain behaviour is defined by Hooke's law by means of Young's modulus  $E$  and Poisson's ratio  $\nu$  (under plane stress):

$$\begin{bmatrix} \sigma_{11} \\ \sigma_{22} \\ \sigma_{12} \end{bmatrix} = \frac{E}{1 - \nu^2} \begin{bmatrix} 1 & \nu & 0 \\ \nu & 1 & 0 \\ 0 & 0 & \frac{1 - \nu}{2} \end{bmatrix} \begin{bmatrix} \varepsilon_{11} \\ \varepsilon_{22} \\ \varepsilon_{12} \end{bmatrix} \quad (13)$$

## 3 RESULTS

### 3.1 Montevideo Splitting Test

The novel 2,5D simulation method was first evaluated using the Montevideo Splitting Test (MVD). The following data were adopted from previous research [8, 13]: mesostructure images taken from three sections (S1-S3), specimen measurements of 70x70x70 mm ( $W \times H \times L$ ), boundary conditions (Figure 5), and material parameters ( $G_F$  is a fracture energy) for bulk and cohesive elements (as listed in Tables 1-2).

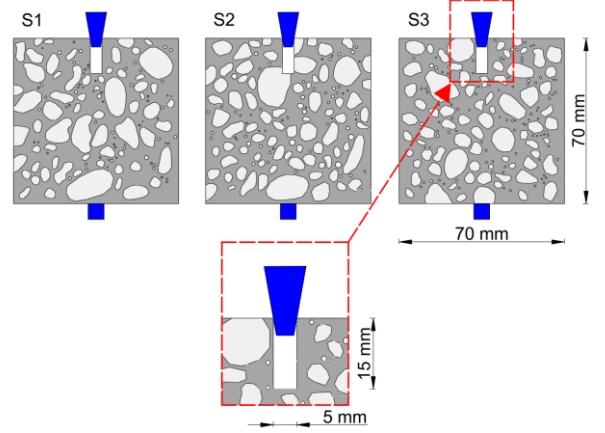


**Figure 5:** Single 2D MVD models for different mesostructures (S1-S3) and notch geometry.

**Table 1:** Material parameters for bulk elements for MVD model

parameter	aggregate	cement matrix	steel
$E$ [GPa]	40	20	200
$\nu$ [-]	0.2	0.2	0.3

**Table 2:** Material parameters for cohesive elements for MVD model

parameter	cem-cem interfaces	ITZ interfaces
$k_{n0} = k_{s0}$ [MPa/mm]	$10^6$	$10^6$
$\alpha$ [-]	7.5	7.5
$f_t$ [MPa]	3.5	1.75
$G_F$ [N/m]	70	35

In this model specimen is supported by steel flat bar, while the load application is applied through a steel wedge acting directly on a 5x15 mm notch.

Figure 6 presents obtained crack patterns for different sections with stiffness  $k_i$  taken as  $10^2$  MPa, while results with the stiffness  $k_i$  equal to  $10^{12}$  MPa are depicted in Figure 7 (for a sake of simplicity, the thickness  $t$  was assumed to be equal to 1.0 m (see Equation (1)).

For relatively low  $k_i$  stiffness values, up to  $10^{10}$  MPa, the results show almost complete convergence with standalone 2D models. However, as the stiffness increases, a significant enhancement in the interaction between the connected planes is observed, highlighting the crucial role of stiffness in the

behaviour of the system under 2.5D analysis. It should be noted that too large stiffness  $k_i$  arrests the formation of cracks in all sections and, in consequence, no softening in force-displacement curve is produced.

### 3.2 Three-point bending test

The three-point beam bending test (TPBT) was utilized as a second benchmark for the proposed method. The images of the mesostructure from three different sections S1-S3, the geometric dimensions of the specimen 40x80x320 mm ( $W \times H \times L$ ), boundary conditions (Figure 8), and the parameters for bulk and cohesive materials (Table 3-4) have been taken from previous studies by Trawiński et al. [4].

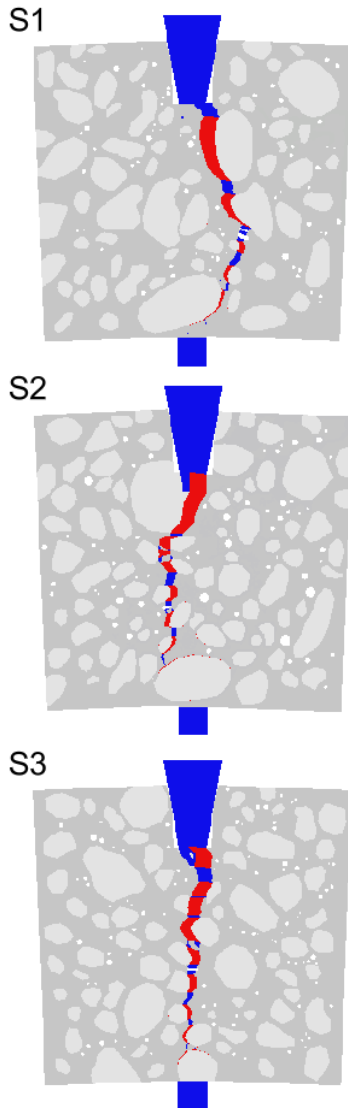


**Figure 6:** MVD 2,5D model crack patterns results set for sections S1-S3 ( $k_i = 10^2$  MPa).

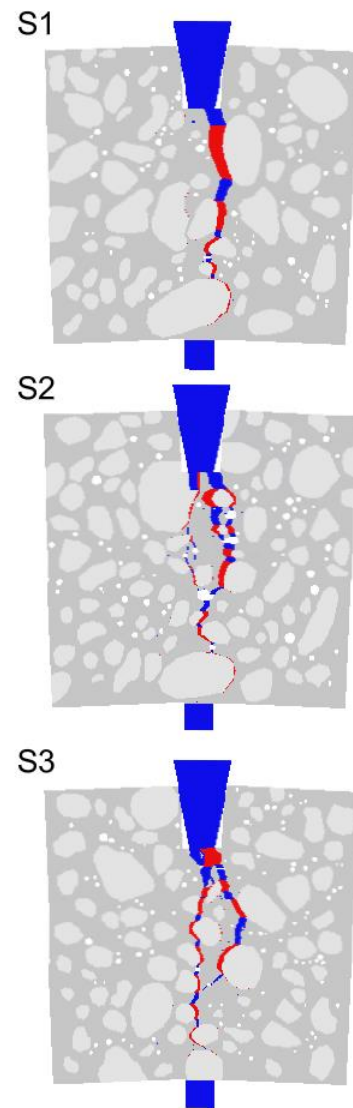


**Figure 7:** MVD 2,5D model crack patterns results set for sections S1-S3 ( $k_i = 10^{12}$  MPa).



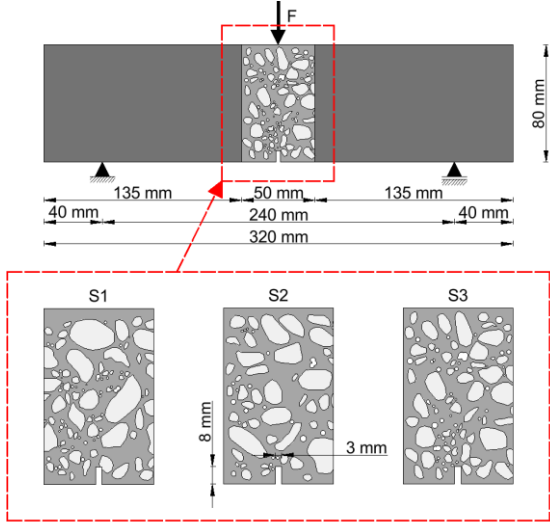


**Figure 8:** Single 2D beam model geometry and three different real mesostructures S1-S3.

Consistent with studies in [4], a two-scale model is employed, wherein a 4-phase mesoscale model is distinguished in the central region, where the expected occurrence of stress concentration induced by the 3x8 mm notch is anticipated, along with the remaining homogeneous part of the beam.

**Table 3:** Material parameters for bulk elements for TPBT model

parameter	aggregate	cement matrix	homog. part
$E$ [GPa]	47.2	29.2	36.1
$\nu$ [-]	0.2	0.2	0.2

**Table 4:** Material parameters for cohesive elements for TPBT model

parameter	cem-cem interfaces	ITZ interfaces
$k_{n0} = k_{s0}$ [MPa/mm]	$10^6$	$10^6$
$\alpha$ [-]	7.5	7.5
$f_t$ [MPa]	4.4	1.6
$G_F$ [N/m]	40	20

Obtained results are shown in Figure 9 (stiffness  $k_i$  taken as  $10^2$  MPa) and Figure 10 (stiffness  $k_i$  equal to  $10^{12}$  MPa). Similar conclusions as before can be drawn. With small spring stiffnesses, almost independent sections behaviour is observed, while usage of larger stiffness values cause modification of crack pattern observed in each section.

## 4 SUMMARY

The new approach to simulate concrete and reinforced concrete specimens has been proposed. The 2.5D model is formed as a set of 2D planes with spring connections between neighbouring ones. It enables the execution of 2D calculations while accounting for various topology configurations in individual cuts and the interactions between plane models. Preliminary results have confirmed the ability of this idea to reproduce the 3D character of the analysed specimens.

The future research will be concentrated on the detailed comparison between 2D, 2.5D and 4D simulations. In order to properly define all three models (based on the same mesostructure), a 3D mesostructure generator is currently developed with the possibility to extract 2D cuts. It will also enable the comparison of computational time efficiency across all approaches.

## ACKNOWLEDGEMENTS

Computations were carried out using the computers of the Centre of Informatics Tricity Academic Supercomputer & Network. This research was partially funded by the National Centre for Research and Development and Clean Energy Transition Partnership (CETP) co-funded by the European Union within project WECHULL+ “Sustainable Concrete Material Leading to Improved Substructures for Offshore Renewable Energy Technologies” (CETP-2022-00127).

## REFERENCES

- [1] J. Tejchman, J. Bobiński, 2013. *Continuous and Discontinuous Modelling of Fracture in Concrete Using FEM*. Springer Berlin Heidelberg.
- [2] M. Szczecina, P. Tworzewski, I. Uzarska, 2018. Numerical modeling of reinforced concrete beams, including the real position of reinforcing bars. *Structure and Environment* **10**.
- [3] M. Pazdan, 2021. FEM modelling of the static behaviour of reinforced concrete

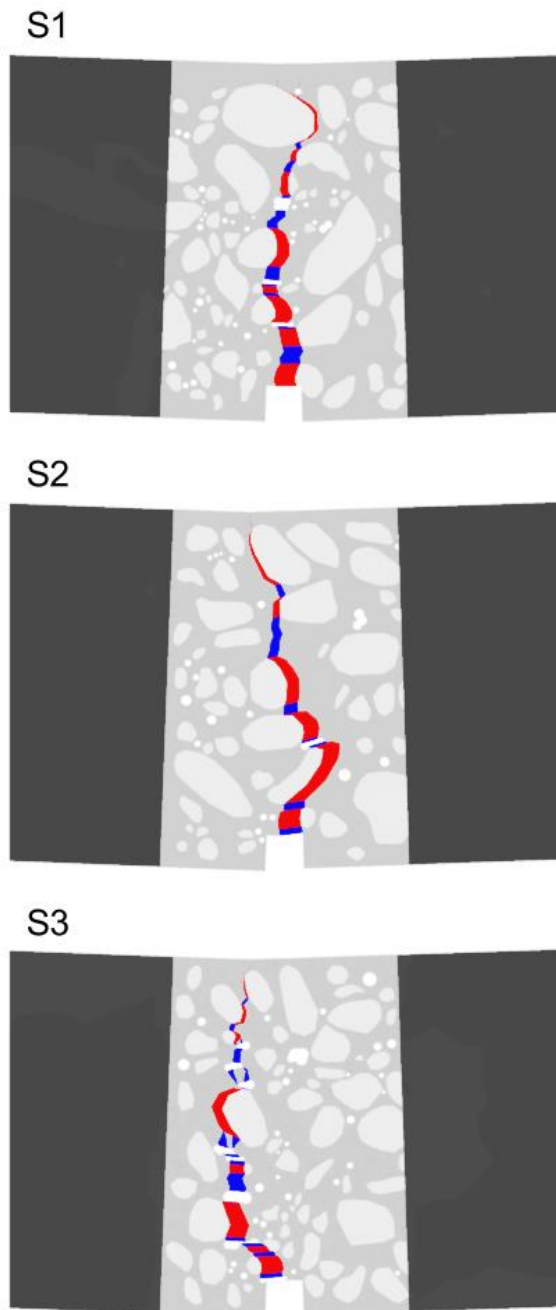


**Figure 9:** TPBT 2,5D model crack patterns results set for sections S1-S3 ( $k_i = 10^2$  MPa).

beams considering the nonlinear behaviour of the concrete. *Studia Geotechnica et Mechanica* **43**:206–223.

- [4] W. Trawiński, J. Bobiński, J. Tejchman, 2016. Two-dimensional simulations of concrete fracture at aggregate level with cohesive elements based on X-ray  $\mu$ CT images. *Engineering Fracture Mechanics* **168**:204–226.

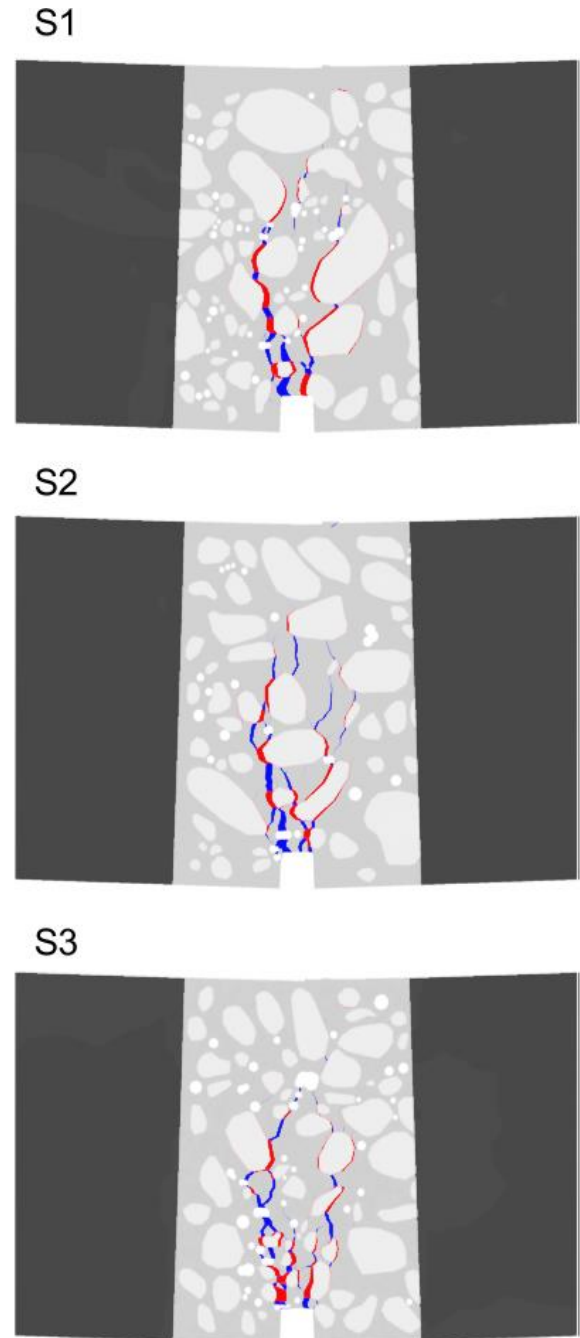


**Figure 10:** TPBT 2,5D model crack patterns results set for sections S1-S3 ( $k_i = 10^{12}$  MPa).

- [5] W. Trawiński, J. Tejchman, J. Bobiński, 2018. A three-dimensional meso-scale modelling of concrete fracture, based on cohesive elements and X-ray  $\mu$ CT images. *Engineering Fracture Mechanics* **189**:27–50.
- [6] J. Wang, A.P. Jivkov, D.L. Engelberg, Q.M. Li, 2018. Meso-scale modelling of mechanical behaviour and damage

evolution in normal strength concrete. *Procedia Structural Integrity* **13**:560–565.

- [7] X. Wang, A.P. Jivkov, 2015. Combined Numerical-Statistical Analyses of Damage and Failure of 2D and 3D Mesoscale Heterogeneous Concrete. *Mathematical Problems in Engineering* **2015**:1–12.
- [8] B. Kondys, J. Bobiński, I. Marzec, 2023. Non-uniqueness of fracture parameter choice in simulations of concrete cracking at mesoscale level. *Archives of Mechanics* **75**:365–396.
- [9] H. Chen, B. Xu, J. Wang, X. Nie, Y.-L. Mo, 2020. XFEM-Based Multiscale Simulation on Monotonic and Hysteretic Behavior of Reinforced-Concrete Columns. *Applied Sciences* **10**:7899.
- [10] L. Jin, X. Li, R. Zhang, X. Du, 2022. Modelling of bond behavior of deformed bar embedded in concrete after heating to high temperatures: A mesoscale study. *Construction and Building Materials* **334**:127456.
- [11] T.J. Truster, 2018. DEIP, discontinuous element insertion Program — Mesh generation for interfacial finite element modeling. *SoftwareX* **7**:162–170.
- [12] A. Hillerborg, M. Modéer, P.-E. Petersson, 1976. Analysis of crack formation and crack growth in concrete by means of fracture mechanics and finite elements. *Cement and Concrete Research* **6**:773–782.
- [13] B. Kondys, J. Bobiński, I. Marzec, 2022. Numerical investigations of discrete crack propagation in Montevideo splitting test using cohesive elements and real concrete micro-structure. W *Computational Modelling of Concrete and Concrete Structures*. CRC Press, London, pp.107–116.